

UNIFIED METHODOLOGY FOR STRENGTH AND STRESS ANALYSIS OF STRUCTURAL CONCRETE MEMBERS

Nazar OUKAILI

Department of Civil Engineering, University of Baghdad, IRAQ
E-mail: nazar.oukaili@coeng.uobaghdad.edu.iq

In this paper, a methodology is presented for determining the stress and strain in structural concrete sections, also, for estimating the ultimate combination of axial forces and bending moments that produce failure. The structural concrete member may have a cross-section with an arbitrary configuration, the concrete region may consist of a set of subregions having different characteristics (i.e., different grades of concretes, or initially identical, but working with different stress-strain diagrams due to the effect of indirect reinforcement or the effect of confinement, etc.). This methodology is considering the tensile strain softening and tension stiffening of concrete in addition to the tension stiffening of steel bars due to the tensile resistance of the surrounding concrete layer. A comparison of experimental and numerical data indicates that the results, obtained based on this methodology, are highly reliable and highly informative.

Keywords: curvature, secant modulus, uniaxial stress-strain, extinction of prestressing, cracking, deformability.

1. Introduction

The adopted assumptions for the analysis of reinforced, partially, and fully prestressed concrete flexural members, based on the normative approaches of the ACI 318-19 [1], AASHTO [2], IBC [3], Eurocode 2 [4], BS-8110 [5], AS3600 [6], and CSA A23.3 [7] are identical and lead to fairly acceptable results for the ultimate steel stresses and the load-carrying capacity. These approaches use the no-slip bending theory and neglect the tensile resistance of concrete and bond-slip. These assumptions, however, yield an erroneous prediction of the member axial strain and curvatures at loading stages above the service load.

In 1908, Mörsch [8] explained that cracked concrete can decrease strain in steel due to tensile stresses in the concrete between cracks. This phenomenon was later called “tension stiffening”. As a result, the stiffness of the beam varies along its length even in a zone of constant bending moment. So, the stiffness is minimum at the crack positions, whilst it increases between cracks due to the contribution of the concrete in tension.

Accordingly, the actual behavior of the structural member is stiffer, due to the capability of concrete to transmit stresses in tension even after cracking begins. It is well known that neglecting the tensile resistance of concrete, usually adopted in ultimate load calculations, leads to a significant overestimation of the values of the strain vector components and as a result the displacements of the structural member. The degree of error depends on the steel percentage and increases as the steel percentage decreases. Beeby [9] reported that with beams having 0.75% tension reinforcement, the error in the calculated deflections at working loads will be in the order of 100%.

To consider this stiffening, three different effective mechanisms should be accounted, namely, (1) the tensile strain-softening phenomenon of concrete, i.e., the fact that, after reaching the concrete strength limit, the tensile stress does not drop suddenly to zero but decreases gradually as the strain increases (Jenn-Chuan *et al.* [10]), (2) the tension stiffening phenomenon of steel bars due to the tensile resistance of concrete layer surrounding the bar, which is forced by bond stresses to extend simultaneously with the bar (i.e., the uncracked concrete which exists between cracks in the tension zone, contributes to the stiffness of the member) (Jenn-Chuan *et al.* [10]; Alameh and Harajli [11]), and (3) the tension stiffening phenomenon of concrete, i.e., the argument that, after cracking, the concrete tensile stresses below the neutral axis position above the tip of the crack are not zero as conventionally

assumed (Alameh and Harajli [11]). A summary of research carried on tension stiffening and cracking of structural concrete in direct tension is given by different works (ACI Committee 224 [12]; CEB [13]).

There are two main reasons behind the fact that the phenomenon of the strain-softening should be considered, namely (1) the crack bridging achieved by pieces and fragments of aggregate that are still anchored at both sides of the crack surface, and (2) the cracks that initiate to appear at the concrete strength limit are discontinuous in nature and do not become continuous until the strain increases progressively and the stress gets declined to zero (Jenn-Chuan *et al.* [10]). While, the main reason behind the tension stiffening phenomenon is that the intact concrete in the tension zone of the section which is located between two adjacent cracks can still develop significant tensile stresses after cracking, due to the bond between steel bars and the surrounding concrete, to contribute to the flexural stiffness of the concrete beam. Such a tension stiffening effect in a flexural member is not quite the same as that in an axial member because the tensile stresses in a cracked flexural member are induced not only by the steel reinforcement–concrete bond but also by the curvature of the flexural member (Ng *et al.* [14]).

The existing tension stiffening theory adopted the assumption which stated that the tensile stress of concrete falls suddenly to zero as soon as the concrete tensile ultimate strength is attained, and that continuous tension-free cracks, normal to the axis of the bar, appear immediately at a certain spacing as the principal tensile stress from restraint forces exceeds the tensile ultimate strength of concrete. It is worth mentioning that the continuous tension-free cracks can be expected to form only after a large increase of strain in the steel occurs because part of the bar force is assumed to be transmitted to the concrete between two adjacent cracks by bond stresses (and, conversely, the tensile resistance of concrete between these cracks restrains the tensile steel bar against axial elongation and increases its stiffness) (Jenn-Chuan *et al.* [10]).

The evaluation of the stress, strain, curvature, and deflection before and after cracking and the estimation of the load-carrying capacity for the structural concrete members have been extensively treated by Nilson [15], Branson and Trost [16, 17], Tadros [18], Bazant and Oh [19], Tadros *et al.* [20], Kawakami *et al.* [21], Alameh and Harajli [11], Ghali [22], Kawakami and Ghali [23, 24], Mast [25], Bischoff [26, 27], and Bischoff and Scanlon [28]. None of the approaches proposed in those studies considered all the three mentioned above stiffening mechanisms. Failing to account for the three mechanisms in modeling the response of the structural concrete member will lead to incorrect and unrealistic results. However, the fully consistent methodology for the analysis of structural concrete members should take into account the three mechanisms together because an acceptable agreement with test results can be achieved only when all mechanisms are taken into account.

2. Uniaxial stress-strain diagrams for materials

Many different analytical expressions have been proposed that more or less accurately describe the deformation of concrete under compression, with or without the descending branch, as well as for mild and high strength steel (Scordelis [29]; Oukaili [30]). A review of the analytical constitutive relationships for concrete and steel reinforcement, with a detailed description of their competency, weaknesses, and powerful aspects, was given in the literature (Oukaili [30]; Popovics [31]; Naaman [32]; Karpenko *et al.* [33]). Relationships proposed by Karpenko *et al.* [33, 34], which were originally developed considering most of the deficiencies, became widespread in the 1990s. In this study, the short-term uniaxial stress-strain diagram adopted for the concrete and steel is based on these relationships.

Let f_m denote stress, ε_m – strain, E_m – initial modulus of elasticity, and let m denote the general index which describes the type of material under consideration. This index shows that the parameter or relationship to concrete or to steel, where $m = (c)$ or (ct) for concrete under uniaxial compression or uniaxial tension, respectively. While $m = (s)$ or (ps) for mild steel or high strength prestressed steel, respectively, under uniaxial tension or compression. Instead of f_m and ε_m , it is more convenient to operate with their levels, so

$$\tilde{f}_m = \left| \frac{f_m}{\hat{f}_m} \right| ; \quad \tilde{\varepsilon}_m = \left| \frac{\varepsilon_m}{\hat{\varepsilon}_m} \right| \quad (2.1)$$

where \hat{f}_m and $\hat{\varepsilon}_m$ – are the stress at the vertex of the stress-strain diagram and its corresponding strain. At the beginning of the stress-strain diagram, (mainly for steel), a linear portion which extends up to the stress $f_{m,el}$ and strain $\varepsilon_{m,el}$ or their levels $\tilde{f}_{m,el}$ and $\tilde{\varepsilon}_{m,el}$ can be distinguished. Nonlinear diagrams are most simply introduced into the elements of the stiffness matrix of the structural members if they are represented as follows:

$$\varepsilon_m = \frac{f_m}{E'_m} = \frac{f_m}{E_m \vartheta_m} \quad (2.2)$$

where E'_m is the secant modulus of elasticity; and ϑ_m is the coefficient of elasticity, (i.e., coefficient of changing of the secant modulus), which represents the ratio of elastic strain to the total strain.

From the different types of stress-strain diagrams (Fig.1.), the coefficient of elasticity (ϑ_m) can be expressed in a uniform shape:

$$\vartheta_m = \begin{cases} 1, & |f_m| \leq |f_{m,el}| \\ \hat{\vartheta}_m \pm (\vartheta_o - \hat{\vartheta}_m) \sqrt{1 - e_m \eta_m - (1 - e_m) \eta_m^2}, & |f_m| > |f_{m,el}| \end{cases} \quad (2.3)$$

where η_m is the stress level ($0 \leq \eta_m \leq 1$); ϑ_o is the value of the coefficient of elasticity ϑ_m at the onset of the stress-strain diagram; $\hat{\vartheta}_m$ is the value of the coefficient of elasticity ϑ_m at the vertex of the stress-strain diagram; and e_m is the diagram curvature parameter

$$\eta_m = \frac{f_m - f_{m,el}}{\hat{f}_m - f_{m,el}} = \frac{\tilde{f}_m - \tilde{f}_{m,el}}{1 - \tilde{f}_{m,el}} \quad (2.4)$$

From the condition of definability of Eq.(2.3), it follows that $e_m \leq 2$. Also, the sign (+) corresponds to the ascending branch and the sign (-) to the descending branch of the stress-strain diagram.

Based on Eqs.(2.1)-(2.2), \tilde{f}_m can be determined as follows:

$$\tilde{f}_m = \frac{\tilde{\varepsilon}_m \vartheta_m}{\hat{\vartheta}_m} \quad (2.5)$$

As $\varepsilon_m > \varepsilon_{m,el}$, the quadratic Eq.(2.3) can be transformed to take the following shape:

$$\begin{aligned} & \vartheta_m^2 \left[1 + \frac{(1 - e_m)(\vartheta_o - \hat{\vartheta}_m)^2 \tilde{\varepsilon}_m^2}{\hat{\vartheta}_m^2 (1 - \tilde{f}_{m,el})^2} \right] - \vartheta_m \left[2 \hat{\vartheta}_m - \frac{\tilde{\varepsilon}_m (\vartheta_o - \hat{\vartheta}_m)^2}{\hat{\vartheta}_m (1 - \tilde{f}_{m,el})} \left\{ e_m - \frac{2(1 - e_m) \tilde{f}_{m,el}}{(1 - \tilde{f}_{m,el})} \right\} \right] + \\ & + \hat{\vartheta}_m^2 - (\vartheta_o - \hat{\vartheta}_m)^2 \left[1 + \frac{e_m \tilde{f}_{m,el}}{(1 - \tilde{f}_{m,el})} - \frac{(1 - e_m) \tilde{f}_{m,el}^2}{(1 - \tilde{f}_{m,el})^2} \right] = 0 \quad (2.6) \end{aligned}$$

Thus, the determination of ϑ_m through the strain level $\tilde{\epsilon}_m$ also leads to the solution of a quadratic equation, the greater roots of Eq.(2.6) should be considered.

2.1. Stress-strain diagrams for concrete

For concrete of different grades, parameters of the functions ϑ_m were determined based on the analysis of extensive experimental data (Karpenko *et al.* [33]).

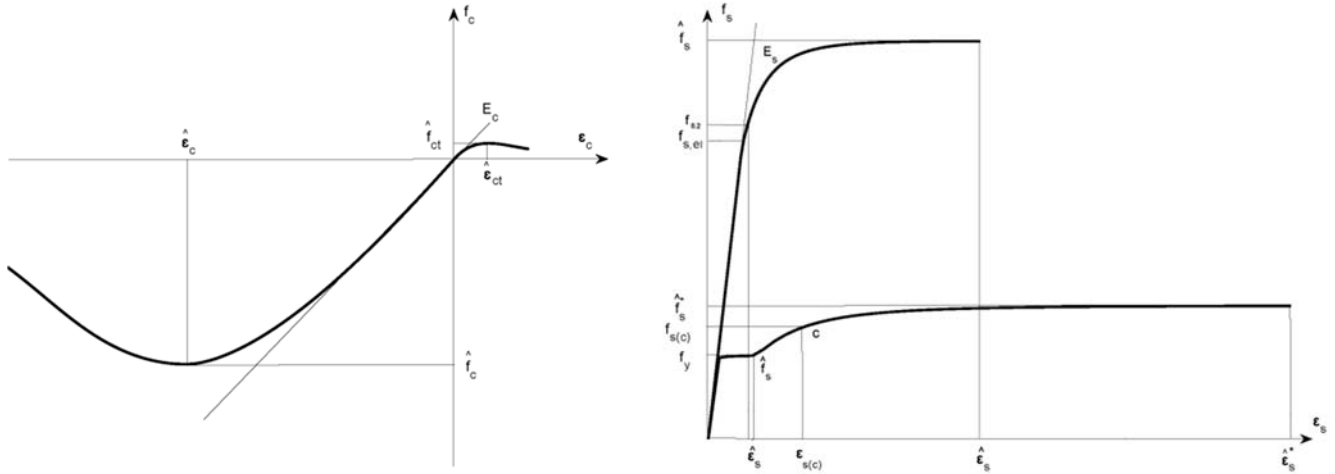


Fig.1. Stress–strain diagrams for concrete and steel.

It has been established that Eq.(2.2) with Eq.(2.3) successfully simulate the experimental stress-strain diagram of normal-weight concrete under uniaxial compression or tension, when these parameters are considered as follows:

$$\hat{\vartheta}_m = \hat{\vartheta}_c = \frac{\hat{f}_c}{|\hat{\epsilon}_c| E_c} \tag{2.7}$$

where

$$f_{m,el} = f_{c,el} = 0; \quad \epsilon_{m,el} = \epsilon_{c,el} = 0$$

and

$$e_m = e_c = \begin{cases} 1.72 - 1.82 \hat{\vartheta}_c, & \tilde{\epsilon}_c \leq 1, \\ 1.95 \hat{\vartheta}_c - 0.138, & \tilde{\epsilon}_c > 1, \end{cases} \tag{2.8}$$

$$\vartheta_o = \begin{cases} 1, & \tilde{\epsilon}_c \leq 1, \\ 2.05 \hat{\vartheta}_c, & \tilde{\epsilon}_c > 1. \end{cases} \tag{2.9}$$

2.2. Stress-strain diagram for steel

To depict the stress-strain diagram for steel under uniaxial tension or compression, in addition to the above-mentioned characteristics (E_s , $f_{s,el}$, \hat{f}_s and $\hat{\varepsilon}_s$), the physical or the proof stress $f_{0.2}$, its corresponding strain $\varepsilon_{0.2}$, and the elasticity coefficient $\vartheta_{0.2}$ should be also used

$$\varepsilon_{0.2} = \frac{f_{0.2}}{E_s} + 0.002, \quad (2.10)$$

$$\vartheta_{0.2} = \frac{f_{0.2}}{E_s \varepsilon_{0.2}} \quad (2.11)$$

where $f_{0.2}$ is the proof stress of high strength steel determined by 0.2% set method; $\varepsilon_{0.2}$ is the strain corresponding to the proof stress $f_{0.2}$ of high strength steel; $\vartheta_{0.2}$ is the coefficient of elasticity of steel corresponding to the stress $f_{0.2}$ and strain $\varepsilon_{0.2}$; $f_{s,el}$ is the steel elastic limit ($f_{s,el} = \beta_{el} f_{0.2}$); and β_{el} is the coefficient of proportional limit.

Based on these characteristics, the unknown parameter e_s is determined from the following expression:

$$e_s = \frac{(\vartheta_o - \hat{\vartheta}_s)^2 (\eta_{0.2}^2 - 1) + (\vartheta_{0.2} - \hat{\vartheta}_s)^2}{(\eta_{0.2}^2 - \eta_{0.2})(1 - \hat{\vartheta}_s)^2} \leq 2 \quad (2.12)$$

in which

$$\vartheta_o = 1; \quad \hat{\vartheta}_s = \frac{\hat{f}_s}{E_s \hat{\varepsilon}_s}; \quad \eta_{0.2} = \frac{f_{0.2}}{\hat{f}_s} \frac{f_{0.2} - f_{s,el}}{f_{0.2} - f_{s,el} f_{0.2} / \hat{f}_s}. \quad (2.13)$$

For the mild steel with physical yielding plateau, \hat{f}_s and $\hat{\varepsilon}_s$ are considered to be conditional. They are corresponding to the stress and strain at the end of the yielding plateau, which can be adopted as:

$$\hat{f}_s = (1.01 \sim 1.03) f_y; \quad \hat{\varepsilon}_s = \hat{f}_s / E_s + \lambda_y; \quad f_{0.2} = 0.99 f_y; \quad \beta_{el} = 0.97 \quad (2.14)$$

where f_y is the yield strength of mild steel; and λ_y is the length of the yielding plateau that depends on the grade of steel (Karpenko *et al.* [33]).

When the steel strain enters the strength hardening zone, it is recommended to use two paired diagrams. The first one, that is described above, terminates at the end of the yielding plateau, (with $f_s = \hat{f}_s$ and $\varepsilon_s = \hat{\varepsilon}_s$), and the second diagram – continues the first one and terminates at a point, (with $f_s = \hat{f}_s^*$ and $\varepsilon_s = \hat{\varepsilon}_s^*$), that corresponds to the rupture of the steel.

The second part of the stress-strain diagram of mild steels can also be described using Eqs.(2.2), (2.3), (2.6), and (2.12) taking into consideration the following:

$$\tilde{f}_s = \frac{f_s}{\hat{f}_s^*}; \quad \tilde{\epsilon}_s = \frac{\epsilon_s}{\hat{\epsilon}_s^*}; \quad \hat{\vartheta}_s = \frac{\hat{f}_s^*}{E_s \hat{\epsilon}_s^*}; \quad \vartheta_o = \frac{\hat{f}_s}{E_s \hat{\epsilon}_s}. \quad (2.15)$$

Also, introduce to the second part of the stress-strain diagram of mild steel an additional point (c) with coordinates:

$$f_{s(c)} = 1.2 f_y; \quad \epsilon_{s(c)} = \frac{f_{s(c)}}{E_s} + 0.05. \quad (2.16)$$

Additionally, the following terms in Eqs.(2.4), (2.11), and (2.13) should be replaced

$$\frac{\tilde{f}_m - \tilde{f}_{m,el}}{1 - \tilde{f}_{m,el}} \quad \text{by} \quad \frac{f_s - \hat{f}_s}{\hat{f}_s^* - \hat{f}_s},$$

$$\vartheta_{0.2} \quad \text{by} \quad \vartheta_{s(c)} = \frac{f_{s(c)}}{E_s \epsilon_{s(c)}},$$

and

$$\eta_{0.2} \quad \text{by} \quad \eta_{s(c)} = \frac{f_{s(c)} - \hat{f}_s}{\hat{f}_s^* - \hat{f}_s}.$$

3. Proposed methodology

The objective of the analysis may be formulated simply: given a general shape section which includes several subsections depending on the grades of concrete used, geometrical properties of concrete and steel (if the steel is available), prestressing history (if prestressing technique is implemented), main characteristic parameters to describe the actual short-term uniaxial stress-strain relationships for concrete and steel (grade, ultimate strength at compression and tension, elastic limit, ultimate strain, strain corresponding to the maximum stress, initial modulus of elasticity), initial strain in nonprestressed and prestressed steel, and the self-weight of the member; find the strain vector and the corresponding stress in concrete, nonprestressed, and prestressed steel at any stage of loading up to failure.

The formulation of the proposed methodology is based on the following assumptions.

1. The plane cross-sections remain plane after loading and the average strain increment at any point within the section region obeys a linear distribution law.
2. It is believed that the structural concrete member is designed in such a way that the shear and bond failures are excluded. Also, the geometrical nonlinearity is neglected.
3. Each discrete concrete area, steel bar, steel wire, and steel strand in the cross-section of the member is assumed to be under a state of uniaxial stresses.
4. The work of concrete and steel in individual elements is modeled by the stress-strain diagrams, both under uniaxial compression and uniaxial tension, obtained during testing of concrete, (cylinders, cubes or prisms specimens), and steel samples, respectively, according to the required specifications.
5. The total stresses are corresponding to the total strains in concrete and steel through the secant modulus of elasticity. Karpenko relationships will be used to determine its value.
6. The tensile stress in concrete does not drop suddenly to zero after reaching the strength limit but decreases gradually as the strain increases with the progress of loading.

7. The artificially uncracked section located between two adjacent cracks will be considered as the effective cross-section for strain analysis in a cracked member at all loading stages up to failure. While the effective cross-section for stress analysis will be adopted based on the actually cracked section.
8. The prestrain which takes into account all losses in prestressing steel and the strain caused by the shrinkage and creep of concrete in nonprestressed steel is considered to be the initial strains in steel. While the strain due to the shrinkage and creep is considered to be the initial strain in concrete.

3.1. Fundamental formulation of basic solution equations

Let there be some rod-shaped structural concrete member in a natural (not deformed) state, where its cross-section occupies the region Ω . Areas of the region Ω are occupied by concrete Ω_c , nonprestressed steel Ω_s , and prestressed steel Ω_{ps} (Fig.2.)

$$\Omega = \Omega_c \cup \Omega_s \cup \Omega_{ps} . \quad (3.1)$$

Regions Ω_c , Ω_s and Ω_{ps} may consist of subregions with different grades of concrete, nonprestressed, and prestressed steel, respectively

$$\Omega = \bigcup_{i=1}^{kk} \Omega_i \quad (3.2)$$

where $\Omega_i (i = 1, \dots, kk)$ - are the subregions of the region Ω , occupied by sections of the individual elements (Fig.2.).

Apply a system of Cartesian coordinates to the region Ω , the center of which will serve the point of intersection of the longitudinal axis of the member with the plane of the section (i.e., the arbitrary point O).

The global coordinate system xyz is defined by a longitudinal reference axis z , which may not be the centroidal axis. The adopted positive sign direction for forces should satisfy positive tensile strain at points of the section region, including the point lying on the longitudinal reference axis of the element. Also, curvatures with a positive sign will be considered those which are orienting the axis of the element with convexity down and to the left (Fig.2.).

The applied load changes the configuration of the member and causes deformation, where the strain energy per unit length $U^{(\ell)}$ equals:

$$U^{(\ell)} = \frac{1}{2} \int_{\Omega} f \varepsilon ds + \frac{1}{2} \int_{\Omega} \tau \gamma ds \quad (3.3)$$

where τ is the shear stress; and γ is the shear strain.

The basic physical expression are represented as follows:

$$f = E' \varepsilon . \quad (3.4)$$

In Eq.(3.4), the secant modulus of elasticity E' takes the following form:

$$E' = \begin{cases} E'_c & , x, y \in \Omega_c \\ E'_s & , x, y \in \Omega_s \\ E'_{ps} & , x, y \in \Omega_{ps} \end{cases} \quad (3.5)$$

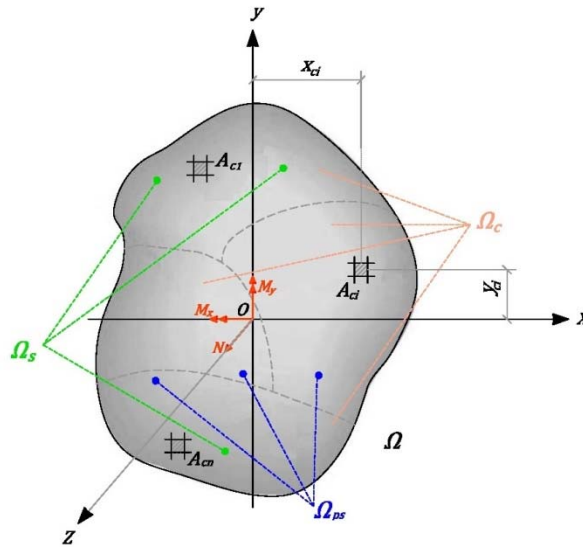
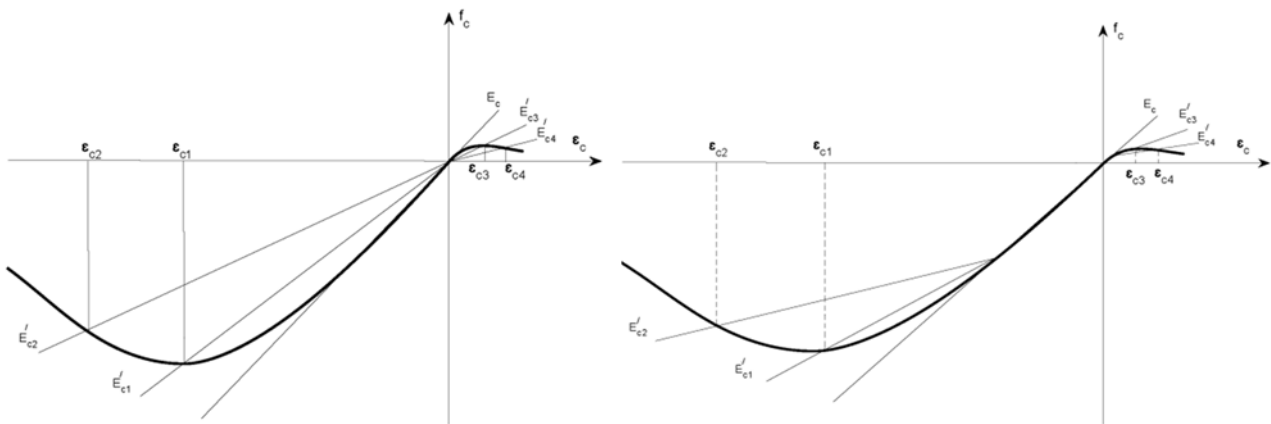


Fig.2. General section shape with positive sign convention.



(a). Secant modulus of elasticity for concrete determined from the beginning of coordinates.

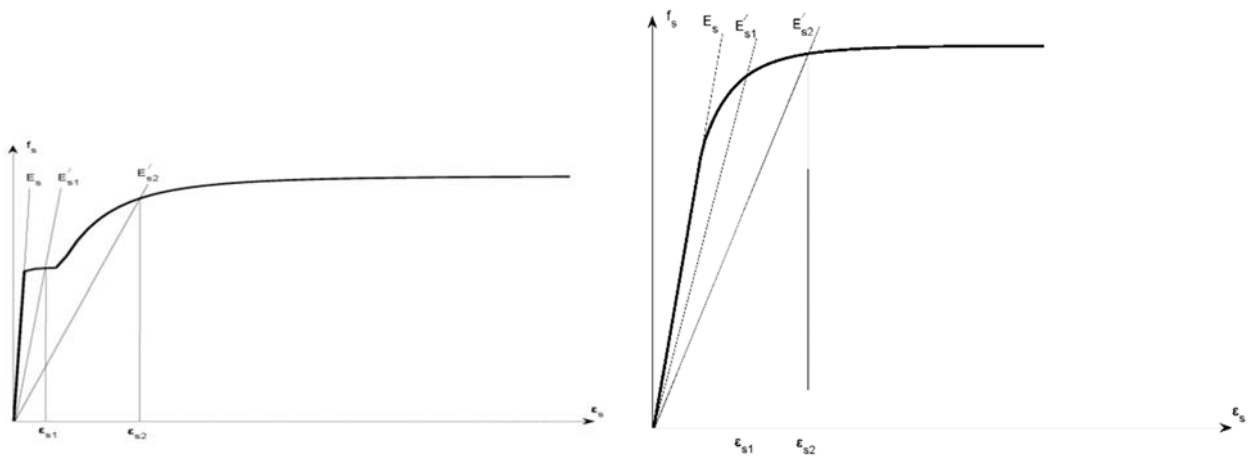
(b). Secant modulus of elasticity for concrete determined from the attained stress stage.

Fig.3. The change of the secant modulus of elasticity for concrete.

Equation (3.5) represents the secant modulus of elasticity for materials, measured from the origin of coordinates of the stress-strain diagram for concrete under compression and tension (Fig.3a.), and for steel (Fig.4a. and Fig.4b.). The secant modulus of elasticity is, as is well known, variable it depends on the achieved stress level, see Fig.3b., Fig.4c., and Fig.4d.

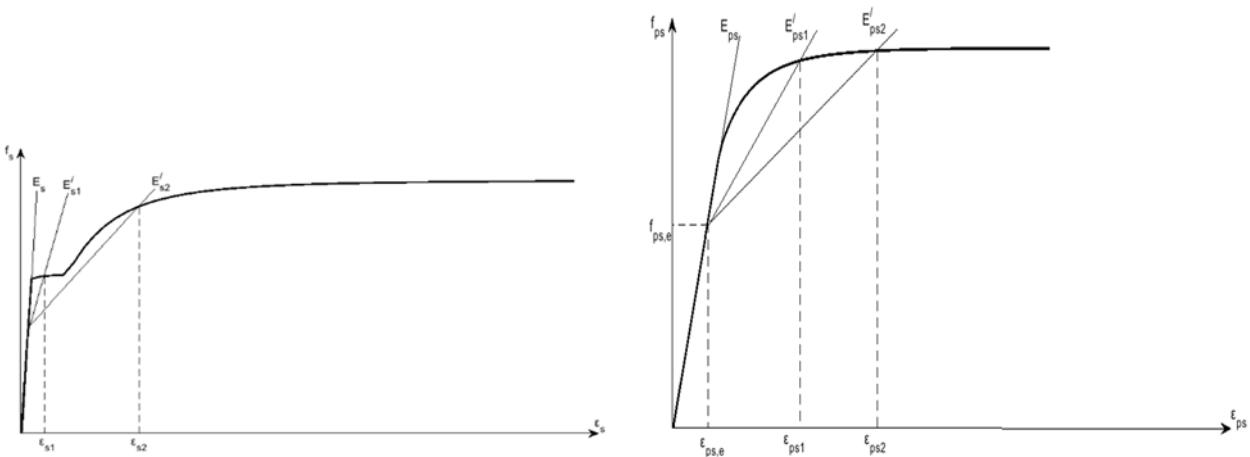
Substituting Eq.(3.4) in Eq.(3.3) and neglecting the second term of Eq.(3.3), Eq.(3.3) takes the following form:

$$U^{(\ell)} = \frac{1}{2} \int_{\Omega} \boldsymbol{\varepsilon} E' \boldsymbol{\varepsilon} ds. \tag{3.6}$$



(a). Secant modulus of elasticity for mild steel determined from the beginning of coordinates.

(b). Secant modulus of elasticity for high strength steel determined from the beginning of coordinates.



(c). Secant modulus of elasticity for mild steel determined from the attained stress stage.

(d). Secant modulus of elasticity for high strength steel determined from the attained stress stage.

Fig.4. The change of the secant modulus of elasticity for steel.

The deformation state of the region Ω can be described by the following expression:

$$\boldsymbol{\varepsilon} = \mathbf{Z}^T \boldsymbol{\lambda}, \quad x, y \in \Omega \tag{3.7}$$

where $\boldsymbol{\lambda}$ and \mathbf{Z} are the finite-dimensional vectors of geometric space,

$$\boldsymbol{\lambda} = (\varepsilon_o \quad \psi_x \quad \psi_y)^T, \tag{3.8}$$

$$\mathbf{Z} = (1 \quad -y \quad -x)^T, \tag{3.9}$$

ε_o is the axial strain at the reference point O ; and ψ_x and ψ_y are the curvature of the member axis in the yz and xz planes, respectively.

The strain vector λ depends on the applied forces (loading level) and the geometric parameters of the cross-section. Equation (3.7) expresses the relationship between the strain of the member reference axis z and the normal strains at any location in the section with coordinates x and y ; it can be rewritten as follow:

$$\varepsilon = \varepsilon_o - \psi_x y - \psi_y x. \quad (3.10)$$

Considering Eq.(3.7), Eq.(3.6) takes a new form:

$$U^{(\ell)} = \frac{1}{2} \int_{\Omega} \lambda^T \mathbf{Z} E' \mathbf{Z}^T \lambda ds. \quad (3.11)$$

The stiffness matrix of the section corresponding to the operator of a static-geometric function is

$$\mathbf{C} = \int_{\Omega} \mathbf{Z} E' \mathbf{Z}^T ds. \quad (3.12)$$

Analyzing Eq.(3.11), it could be concluded that the strain energy per unit length is a function of three variables – i.e., the components of the axial strain vector λ . The partial derivatives of the strain energy per unit length relative to these components will give the associated forces:

$$\left\{ \begin{array}{l} \frac{\partial U^{(\ell)}}{\partial \varepsilon_o} = N_z = \int_{\Omega} E' \mathbf{Z}^T ds \lambda \\ \frac{\partial U^{(\ell)}}{\partial \psi_x} = M_x = \int_{\Omega} -y E' \mathbf{Z}^T ds \lambda \\ \frac{\partial U^{(\ell)}}{\partial \psi_y} = M_y = \int_{\Omega} -x E' \mathbf{Z}^T ds \lambda \end{array} \right\} \quad (3.13)$$

or

$$\left\{ \begin{array}{l} N_z = \mathbf{C}_1 \lambda \\ M_x = \mathbf{C}_2 \lambda \\ M_y = \mathbf{C}_3 \lambda \end{array} \right\} \quad (3.14)$$

where \mathbf{C}_1 , \mathbf{C}_2 , and \mathbf{C}_3 are respectively, generalized axial and flexural stiffness vectors of the section in two directions.

The elements of the vector \mathbf{C}_1 are the axial and the flexural-axial stiffness of the section in two directions

$$\mathbf{C}_1 = \left(\int_{\Omega} E' ds, \quad - \int_{\Omega} y E' ds, \quad - \int_{\Omega} x E' ds \right). \quad (3.15)$$

The elements of the vector C_2 are the flexural-axial, flexural stiffness, and stiffness which takes into account the mutual influence of moments in two directions

$$C_2 = \left(-\int_{\Omega} y E' ds, \int_{\Omega} y^2 E' ds, \int_{\Omega} x y E' ds \right). \quad (3.16)$$

Vector C_3 has the following form:

$$C_3 = \left(-\int_{\Omega} x E' ds, \int_{\Omega} x y E' ds, \int_{\Omega} x^2 E' ds \right). \quad (3.17)$$

Give Eq.(3.14) a more compacted form:

$$F = C\lambda \quad (3.18)$$

where F is the force vector, and C is the stiffness matrix of the section, which is a function of the geometrical and deformational parameters of the cross-section and the applied load

$$F = (N \quad M_x \quad M_y)^T, \quad (3.19)$$

$$[C] = \begin{bmatrix} +C_{11} & -C_{12} & -C_{13} \\ -C_{21} & +C_{22} & +C_{23} \\ -C_{31} & +C_{32} & +C_{33} \end{bmatrix}. \quad (3.20)$$

The direct integration for elements of the stiffness matrix is difficult because the secant modulus of elasticity depends on the strain level, and the gradient of the latter is generally non-zero. Accordingly, it is necessary to resort to elements of numerical integration. For this purpose, the region of the section is covered in the general case by a two-dimensional, more often orthogonal mesh, and, averaging the strains within the boundaries of each elementary area of the mesh, the integral summation is replaced by a finite summation, in which the upper limit is equal to the number of cells of the mesh (Fig.2.).

The concrete cells in the adopted mesh are grouped into kk units with areas A_{ci} ; $i = 1, 2, \dots, kk$. Also, the nonprestressed steel is grouped into mm units with areas A_{sj} ; $j = 1, 2, \dots, mm$. While the prestressing steel is grouped into nn units with areas A_{psk} ; $k = 1, 2, \dots, nn$. Steel reinforcement can be grouped into individual layers in case the section is subjected to uniaxial bending, where the layer shall include steel of the same effective depth, physical-mechanical properties, and prestrain value or initial strain history

$$C_{11} = \sum_{i=1}^{kk} \vartheta_{ci} E_{ci} A_{ci} + \sum_{j=1}^{mm} \vartheta_{sj} E_{sj} A_{sj} + \sum_{k=1}^{nn} \vartheta_{psk} E_{psk} A_{psk}, \quad (3.21)$$

$$C_{12} = C_{21} = -\sum_{i=1}^{kk} \vartheta_{ci} E_{ci} y_{ci} A_{ci} - \sum_{j=1}^{mm} \vartheta_{sj} E_{sj} y_{sj} A_{sj} - \sum_{k=1}^{nn} \vartheta_{psk} E_{psk} y_{psk} A_{psk}, \quad (3.22)$$

$$C_{13} = C_{31} = -\sum_{i=1}^{kk} \vartheta_{ci} E_{ci} x_{ci} A_{ci} - \sum_{j=1}^{mm} \vartheta_{sj} E_{sj} x_{sj} A_{sj} - \sum_{k=1}^{nn} \vartheta_{psk} E_{psk} x_{psk} A_{psk}, \quad (3.23)$$

$$C_{22} = \sum_{i=1}^{kk} \vartheta_{ci} E_{ci} y_{ci}^2 A_{ci} + \sum_{j=1}^{mm} \vartheta_{sj} E_{sj} y_{sj}^2 A_{sj} + \sum_{k=1}^{nn} \vartheta_{psk} E_{psk} y_{psk}^2 A_{psk}, \quad (3.24)$$

$$C_{23} = C_{32} = \sum_{i=1}^{kk} \vartheta_{ci} E_{ci} x_{ci} y_{ci} A_{ci} + \sum_{j=1}^{mm} \vartheta_{sj} E_{sj} x_{sj} y_{sj} A_{sj} + \sum_{k=1}^{nn} \vartheta_{psk} E_{psk} x_{psk} y_{psk} A_{psk}, \quad (3.25)$$

$$C_{33} = \sum_{i=1}^{kk} \vartheta_{ci} E_{ci} x_{ci}^2 A_{ci} + \sum_{j=1}^{mm} \vartheta_{sj} E_{sj} x_{sj}^2 A_{sj} + \sum_{k=1}^{nn} \vartheta_{psk} E_{psk} x_{psk}^2 A_{psk}. \quad (3.26)$$

The stiffness matrix of the cross-section depends on the achieved deformation state, i.e.:

$$\mathbf{F} = \mathbf{C}(\boldsymbol{\varepsilon})\boldsymbol{\lambda}. \quad (3.27)$$

Adding Eq.(3.27) to the Eq.(3.7), the basic solution equations for determining the strength capacity of the section can be obtained

$$\begin{cases} \mathbf{F} = \mathbf{C}(\boldsymbol{\varepsilon})\boldsymbol{\lambda}, \\ \boldsymbol{\varepsilon} = \mathbf{Z}^T \boldsymbol{\lambda}. \end{cases} \quad (3.28)$$

Equation (3.28) can be given a more concise form

$$\mathbf{F} = \mathbf{C}(\boldsymbol{\lambda})\boldsymbol{\lambda}. \quad (3.29)$$

Thus, the system of the third-order nonlinear equations is considered as the tool for determining the stress and strain in structural concrete sections. Also, to estimate the ultimate combination of axial forces and bending moments that produce failure.

3.2. Extinction of prestressing force

In the proposed methodology the prestressing force will be considered as an external factor along with the forces from the external loads, on one hand, and, on the other hand, by shifting the reference point at the stress-strain diagrams of the prestressing steel from the origin (i.e., the zero coordinates) to the point corresponding to the prestress value after all losses (Fig.4c. and Fig.4d.).

In fully and partially prestressed concrete members a process of extinction of prestressing force is proceeding as the applied load is increased beyond a specific level. This is mainly due to the presence on the stress-strain diagram of the prestressing steel nonlinear portions that indicate its inelastic behavior. The process of extinction of prestressing force is a very complicated phenomenon and the present does not have sufficient treatment researches.

To take this fact into account, the normative approaches of the ACI 318-19 [1], AASHTO [2], IBC [3], Eurocode 2 [4], BS-8110 [5], AS3600 [6], and CSA A23.3 [7] suggest the following.

In the serviceability stage, from the point of view that the prestressing steel behaves elastic, the extinction of the prestressing force is not considered and the value of the prestressing force is considered to be a constant value calculated as a product of the effective prestress by the cross-sectional area of the prestressed steel. While, in the ultimate stage of performance, it is considered that there is a complete extinction of the prestressing force (i.e., the prestressing force is assumed to be zero).

In accordance with the proposed methodology, a gradual extinction process for the prestressing force is adopted, since the analysis is carried out by a uniform procedure without any separation between loading stages. Figure 5 illustrates the mechanism of the gradual extinction of the prestressing force adopted in this paper.

The adequate approach to account for the extinction phenomenon can be achieved as follows:

The extinction of prestressing is considered as the "extinction" of the prestressing force, which is calculated, at any loading stage, as a product of the difference between the total stress and the increment of stress by the cross-sectional area of the prestressing steel. At the portion of the stress-strain diagram of the prestressing steel from the onset to the point corresponding to the proportionality limit $f_{ps,el}$, the difference between the total stress and the increment of stress is constant and equals the effective prestress $f_{ps,e}$. On the other part of the diagram from the point corresponding to the proportionality limit $f_{ps,el}$ to the vertex of the diagram \hat{f}_{ps} , this difference decreases gradually resulting in degradation of the effective prestressing force. Accordingly, the components of the force vector will be determined as follows:

$$\left. \begin{aligned} N_z &= N_z + \sum_{k=1}^{nn} (f_{psk} - \Delta f_{psk}) A_{psk} \\ M_x &= M_x + \sum_{k=1}^{nn} (f_{psk} - \Delta f_{psk}) y_{psk} A_{psk} \\ M_y &= M_y + \sum_{k=1}^{nn} (f_{psk} - \Delta f_{psk}) x_{psk} A_{psk} \end{aligned} \right\} \quad (3.30)$$

Here the sign '=' means an assignment, not equality; Δf_{psk} – is the increment of stress in prestressed steel due to the applied external load.

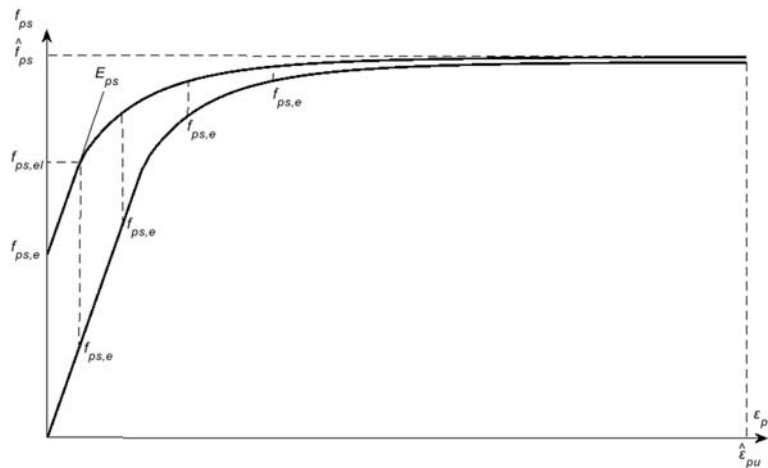


Fig.5. Extinction process of the prestressing force.

Since the second term on the right-hand side of Eq.(3.30) is a variable magnitude which depends on the achieved deformation state of the section, the force vector \mathbf{F} will depend on the strain vector $\boldsymbol{\lambda}$

$$\mathbf{F} = \mathbf{F}(\boldsymbol{\lambda}). \quad (3.32)$$

Considering Eq.(3.31), Eq.(3.29) takes a new form:

$$\mathbf{F}(\boldsymbol{\lambda}) = \mathbf{C}(\boldsymbol{\lambda})\boldsymbol{\lambda}. \quad (3.33)$$

It is worth mentioning that the axial strain and curvatures should be calculated by a step-by-step procedure. In each step, the increments of these variables and the corresponding strains and stresses in concrete and steel are determined based on the previous step. Successive iterations should be used to satisfy equilibrium relations. To solve the systems of nonlinear equations (3.29) and (3.32), an iterative secant method can be used (Douglas and Burden, [35]), the iteration process which has the following form:

$$\begin{cases} \mathbf{F} = \mathbf{C}(\boldsymbol{\lambda}_{i-1})\boldsymbol{\lambda}_i \\ \boldsymbol{\lambda}_0 = 0 \\ i = 1, 2, \dots, \dots \end{cases} \quad (3.33)$$

$$\begin{cases} \mathbf{F}(\boldsymbol{\lambda}_{i-1}) = \mathbf{C}(\boldsymbol{\lambda}_{i-1})\boldsymbol{\lambda}_i \\ \boldsymbol{\lambda}_0 = 0 \\ i = 1, 2, \dots, \dots, \dots \end{cases} \quad (3.34)$$

Here, Eq.(3.33) is used to determine the strength of conventional reinforced concrete sections, while the iterative system (3.34) is used for fully and partially prestressed concrete sections.

3.3. Computer program and algorithm of analysis of the structural concrete members

The matrix nonlinear Eqs.(3.29) and (3.32) for the known external forces N , M_x , and M_y and unknown strain components ε_o , ψ_x , and ψ_y are solved by iterative Eqs.(3.33) or (3.34), depending on the type of the structural concrete member, using the following algorithm which is realized in a computer program:

1. By Eqs.(3.21)-(3.26), the elements of the stiffness matrix for the elastic (unloaded) state in the section are calculated for $\vartheta_{ci} = \vartheta_{sj} = \vartheta_{psk} = I$ (i.e., using $E'_{ci} = E_{ci}$, $E'_{sj} = E_{sj}$, and $E'_{psk} = E_{psk}$, where E_{ci} , E_{sj} , and E_{psk} are the initial moduli of elasticity);
2. Solve Eq.(3.29) or (3.32) to find the strain components ε_o , ψ_x , and ψ_y ;
3. By Eq.(3.10) strains ε_{ci} , ε_{sj} , and ε_{psk} are calculated in all elementary regions A_{ci} , A_{sj} , and A_{psk} ;
4. Based on analytical data of Eq.(2.2), the secant moduli of elasticity E'_{ci} , E'_{sj} , and E'_{psk} are determined for all elementary regions;
5. By Eqs.(3.21)-(3.26), the elements of the stiffness matrix are adjusted;
6. The solution is repeated from point 2.

During the process of these iterative calculations, at a given loading level of external forces N , M_x , and M_y , the values of strain components ε_o , ψ_x , and ψ_y (as the elements of the stiffness matrix are corrected due to the development of inelastic strains in the cross-section) gradually increase, reaching some of their finite (stabilized) values. This is the case if the load-carrying capacity of the adopted cross-section is sufficient to withstand the given external forces. The iterative process, in this case, is considered complete if

the vector of error $\|Z_k\| \rightarrow 0$ when $k \rightarrow \infty$. If the load-carrying capacity of the inspected cross-section is not sufficient to withstand the given external forces, then the strain components ϵ_o , ψ_x , and ψ_y of the iterative calculation process do not stabilize, i.e., these components grow unlimitedly, and consequently, the convergence conditions are not satisfied.

The proposed analysis methodology is extended to determine the load-carrying capacity using the bisection method (Douglas and Burden [35]). The core of this method consists in establishing the interval (F_1, F_2) , in which the solution of the basic Eqs.(3.29) and (3.32) is located. Repeating the iterative process results in a sequence of intervals containing the required vector, where the length of each subsequent interval being half that of the previous one. The iterative process ends when the length of the newly obtained interval becomes less than a given tolerance and the middle of this interval is taken as the required vector.

A general computer program "SECTION" was written in FORTRAN language for this methodology. The program provides a capability for the material nonlinear analysis for general shape cross-sections of various reinforced, partially prestressed, and fully prestressed concrete members. The analysis is considering the tensile strain softening and tension stiffening mechanisms. The program can be used to satisfy the requirements for serviceability and ultimate strength designs. A copy of this program; can be made available for those interested by contacting the author.

4. Verifications and comparison to experimental results

To verify the proposed methodology, numerous examples have been calculated. A massive comparative bank of information has been accumulated for experimental and numerical data of the strength of the section of various configurations, reinforcement, and types of loading (bending, eccentric compression, tension). To evaluate the proposed methodology, comparisons with three groups of static tests conducted by Oukaili [30], Dodonov *et al.* [36, 37], and Bajkov *et al.* [38, 39] on different structural concrete members have been made.

Table 1. Dimensions and materials mechanical properties of tested specimens [30, 36].

Beam ID	Dimensions		Concrete		Prestressed steel				Nonprestressed steel		
	b mm	h mm	\hat{f}_c MPa	E_c MPa	A_{ps} mm ²	E_{ps} MPa	$f_{0.2}$ MPa	$f_{ps,e}$ MPa	A_s mm ²	E_s GPa	$f_{0.2} (f_y)$ MPa
B1	212	302	44.62	32900	193	165350	1587	966	193	165350	1587
B2	213	314	45.29	35750	280	178650	1293	1069	295	191400	998
B3	215	303						1060			
B4	209	302	39.4	32250	420			1031	907	198260	386
B5	210	305						1033			

Table 2. Predicted results of failure moments compared to experimental results [30, 36].

Beam ID	Experimental failure moment	Predicted failure moment according to			
		ACI 318-19 [1]		Proposed methodology	
	M_u^{exp} kN-m	M_u^{cal} kN-m	$\frac{M_u^{cal}}{M_u^{exp}}$ (%)	M_u^{cal} kN-m	$\frac{M_u^{cal}}{M_u^{exp}}$ (%)
B1	128.53	125.88	0.979	125.40	0.976
B2	153.86	151.60	0.985	152.60	0.992
B3	143.81	143.92	1.001	143.80	1.000
B4	181.17	177.26	0.978	172.42	0.952
B5	173.70	181.89	1.047	174.95	1.007
Average of (M_u^{cal} / M_u^{exp})			0.998		0.985
Standard of deviation			0.029		0.022
Coefficient of variation			0.029		0.022

Experimental studies of the strength of partially prestressed concrete members in Oukaili [30] were carried out on beams 3300mm long, with a rectangular cross-section of 200 x 300 mm designed dimensions in a simply supported scheme with an effective span of 3000mm. All specimens were loaded in four-point bending using two symmetrical concentrated loads applied at one-third of the span length. Seven wire strands were used as prestressed steel and different grades of steel reinforcement were used as nonprestressed steel. Table 1 shows the actual dimensions of the tested specimens and the mechanical properties of materials. The load-carrying capacity of the experimental beams was determined using ACI 318-19 [1] and the proposed methodology. Table 2 summarizes the calculated failure moments and their comparisons to the experimental findings.

Results obtained based on this methodology well correlated with the experimental data and not exceeded 5% on average. The experimental values of the failure moments exceed the values calculated by the proposed methodology.

The methodology presented in this paper allows following the stress-strain state and the $(\Delta N - \varepsilon_o)$, $(\Delta M_x - \psi_x)$, and $(\Delta M_y - \psi_y)$ diagrams of the section at all stages of loading up to failure. Figure 6 shows the stress and strain distribution across the section depth, the crack depth during progressive loading, and illustrates $(\Delta M_x - \psi_x)$ diagram for specimen B3.

As can be seen from Table 2, the scatter of the average ratios of the estimated failure moment according to the proposed methodology to the experimental data was 0.985 with a standard deviation of 0.022 and a coefficient of variation of 0.022.

The short column of 1500 mm in length in Dodonov *et al.* [37] with a square cross-section of 200x200 mm dimensions was under eccentric compression force and has the following characteristics: eccentricity of the applied axial force about the x-axis $e_x = 117.2$ mm; the concrete is with $\hat{f}_c = 47.6$ MPa, $\hat{f}_{ct} = 2.20$ MPa, $E_c = 36000$ MPa, $\hat{\varepsilon}_c = 0.0020$; the longitudinal steel reinforcement is four bars class A_T-VII of $\varnothing 20$ mm diameter with $f_{0.2} = 1446$ MPa, $\hat{f}_s = 1600$ MPa, $E_s = 195000$ MPa. The section was divided into 9 strips in the horizontal direction. Figure 7 shows the calculated, based on this methodology, strain, and stress distribution diagrams in concrete and steel. According to the available experimental data, the ultimate axial force was $N_u^{exp} = 860$ kN, while the theoretical value $N_u^{cal} = 880$ kN.

The rectangular cross-section in Bajkov *et al.* [38] was under skew bending moment and has the following characteristics: width $b = 162$ mm, depth $h = 242$ mm, concrete cover $a = 23.5$ mm; the concrete is with

$\hat{f}_c = 21.4MPa$, $\hat{f}_{ct} = 1.58MPa$, $E_c = 21000MPa$, $\hat{\epsilon}_c = 0.0025$; the main steel reinforcement is one bar class A-III_B of $\varnothing 20mm$ diameter with $f_y = 563MPa$, $\hat{f}_s^* = 656MPa$, $E_s = 185500MPa$.

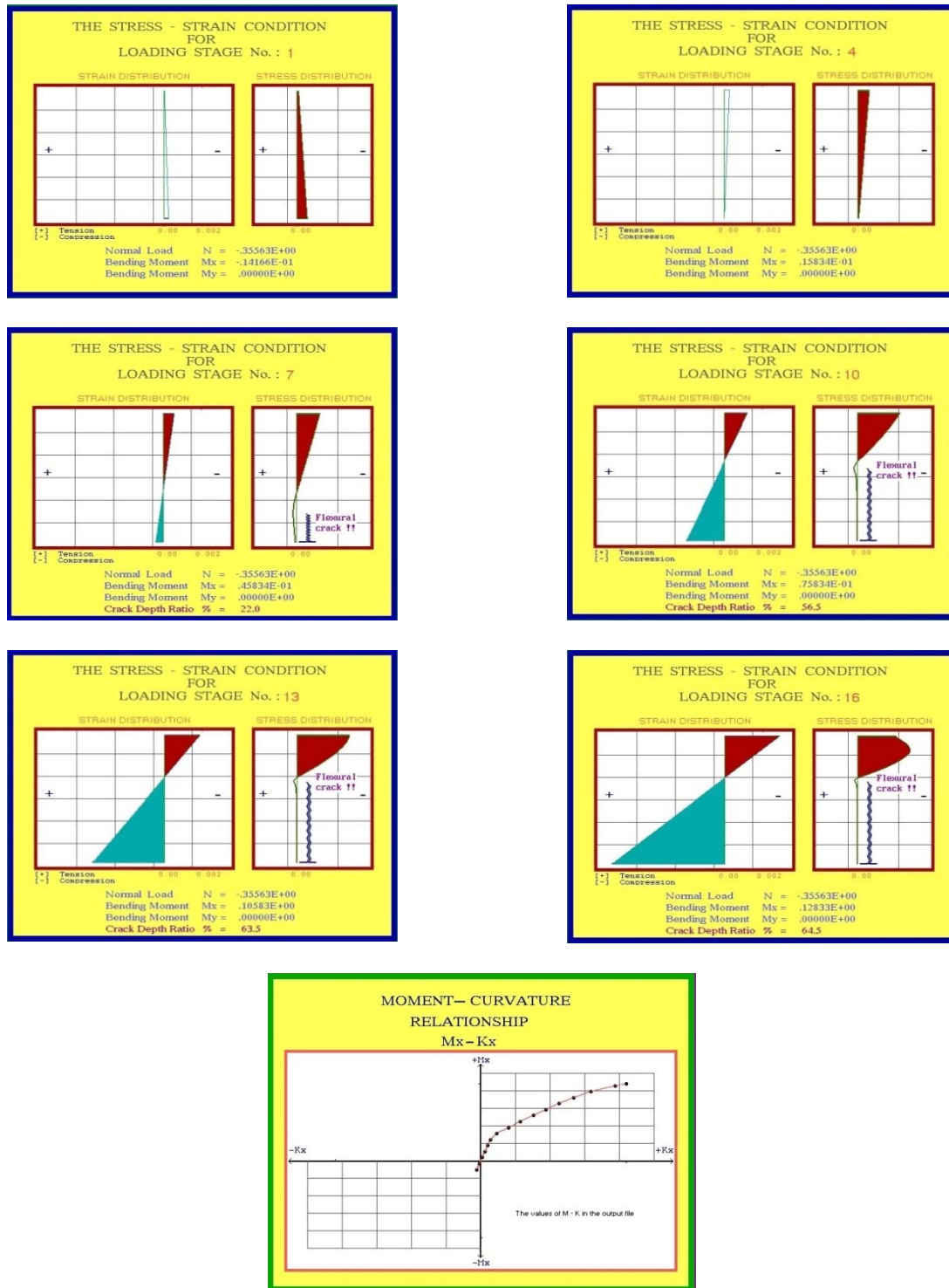


Fig.6. Stress-strain distribution and moment-curvature at different loading stages for specimen B3 [30,36].

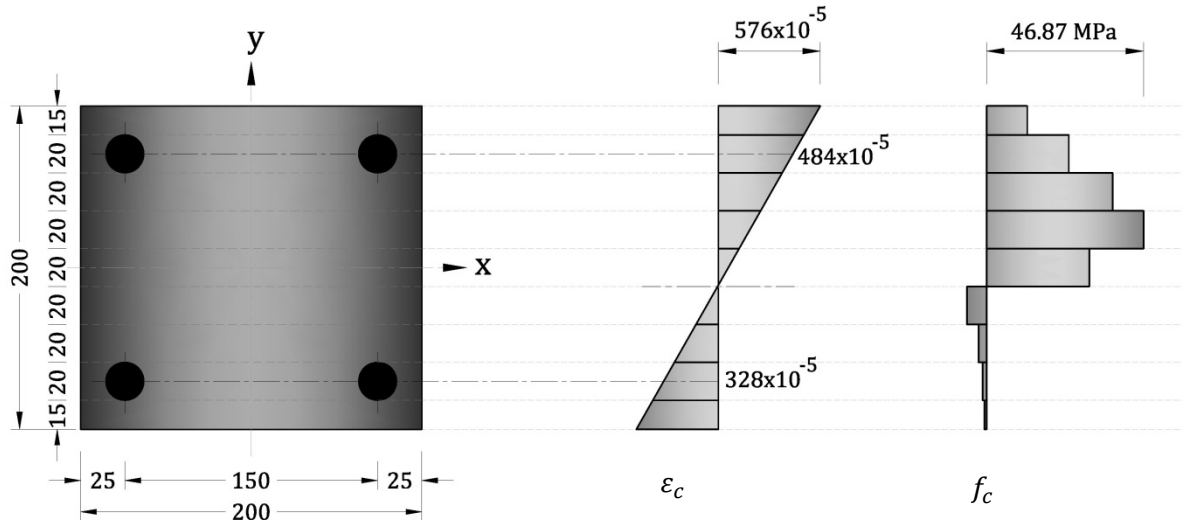


Fig.7. The predicted strain and stress distribution diagrams in concrete and steel in a short column under the eccentric compression force at failure stage [37].

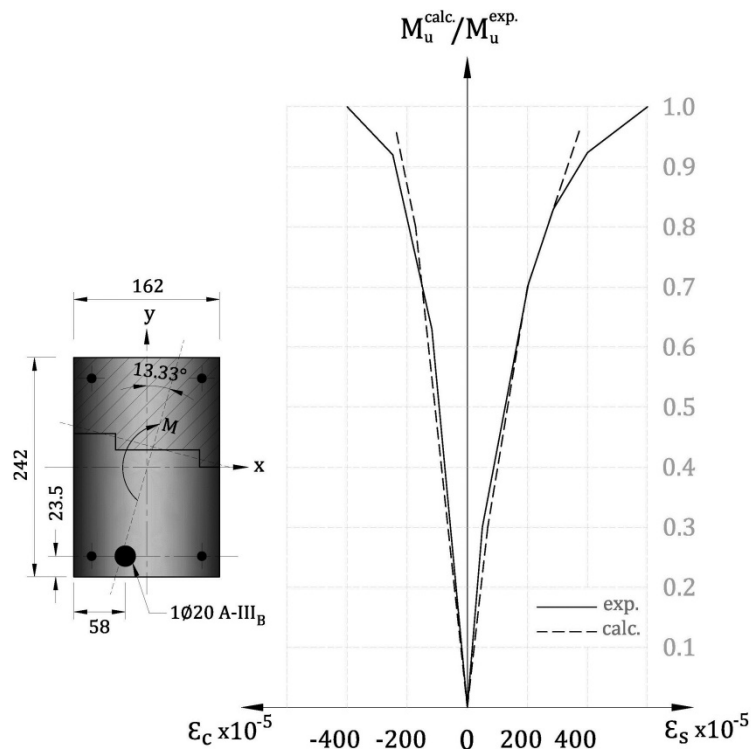


Fig.8. The experimental and calculated load-strain curves in the main steel reinforcement and the most stressed corner in compression zone of the concrete section under skew bending moment at all loading processes [38].

The section was covered by an orthogonal mesh of 154-elementary cells (11 in horizontal and 14 in vertical directions) to investigate the strain in each cell. Figure 8 shows the experimental and calculated load-strain curves in the main steel and the most stressed corner in the compression zone of the section at different loading levels. It is worth mentioning that the experimental ultimate moment was $M_u^{exp} = 36.65 kNm$, while the theoretical value was $M_u^{cal} = 37.66 kNm$.

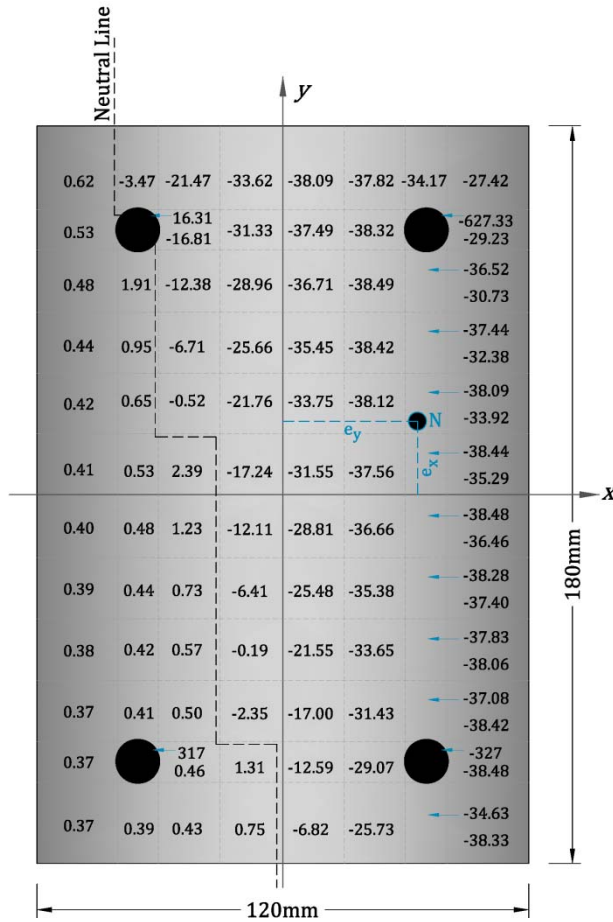


Fig.9. The predicted stresses in the main steel reinforcement and all concrete cells in a short column under skew eccentric compression force at failure stage of loading [39].

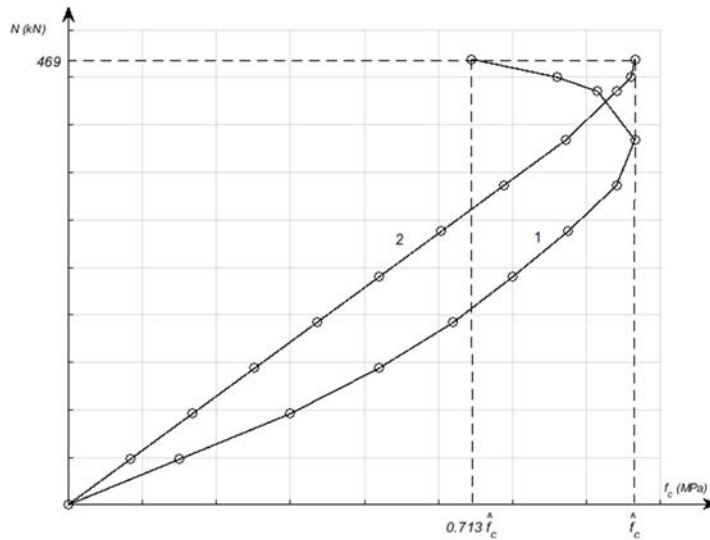


Fig.10. The change of the concrete stress at the top and bottom right corners of the section in a short column under skew eccentric compression force at different stages of loading [39].

The short column of 1200mm length in Bajkov *et al.* [39] with rectangular cross-section was under skew eccentric compression force and has the following characteristics: width $b = 120\text{mm}$, depth $h = 180\text{mm}$, eccentricities of the applied axial force about x-axis and y-axis are $e_x = 17.8\text{mm}$ and $e_y = 33.2\text{mm}$, respectively; the concrete is with $\hat{f}_c = 38.49\text{MPa}$, $\hat{f}_{ct} = 2.46\text{MPa}$, $E_c = 35700\text{MPa}$, $\hat{\epsilon}_c = 0.0025$; the longitudinal steel reinforcement is four bars class A_T-V of $\varnothing 12\text{mm}$ diameter with $f_{0.2} = 1020\text{MPa}$, $\hat{f}_s = 1305\text{MPa}$, $E_s = 190000\text{MPa}$. The section was covered by an orthogonal mesh of 96-elementary cells (8 in horizontal and 12 in vertical directions) to investigate the stress in each cell. Figure 9 shows the calculated stresses in the main steel reinforcement and all concrete cells at the ultimate stage of loading. Meanwhile, Figure 10 illustrates the change of the concrete stress at the top and bottom right corners of the section at different loading stages to show the performance of concrete at the descending branch at the most stressed corner. It is worth mentioning that the experimental ultimate axial force was $N_u^{exp} = 475\text{kN}$, while the theoretical value was $N_u^{cal} = 469\text{kN}$, which was achieved after 36 iterations to get the convergence of the iterative process with an accuracy of 0.001 . All these facts indicate the reliability of the proposed approach.

5. Conclusions

A unified methodology is presented for material nonlinear analysis of the arbitrary shape section of structural concrete rod-shaped members. The system of the third-order nonlinear equations is considered as the tool for determining the stress and strain in structural concrete sections. Also, to estimate the ultimate combination of axial forces and bending moments that produce failure. The stress and strain are determined by an iterative procedure taking into consideration the tensile strain softening and tension stiffening of concrete in addition to the tension stiffening of steel bars due to the tensile resistance of the surrounding concrete layer. The analysis of stress may be extended to determine the crack width and the deflection at any time up to failure. A comparison of the numerical results obtained from the proposed methodology with the experimental findings shows good agreement.

Nomenclature

- a – concrete cover
- A_{ci} – cross-sectional area of the i -th elementary cell of concrete
- A_{psk} – cross-sectional area of the k -th strand, wire or bar of the prestressed steel
- A_{sj} – cross-sectional area of the j -th nonprestressed steel bar
- b – width of the section
- C – stiffness matrix of the section
- C_1 – generalized axial stiffness vectors of the section
- C_2 – generalized flexural stiffness vectors of the section in the x - x direction
- C_3 – generalized flexural stiffness vectors of the section in the y - y direction
- C_{11} – axial stiffness
- C_{12} – flexural-axial stiffness to account for the mutual influence of N and M_x
- C_{13} – flexural-axial stiffness to account for the mutual influence of N and M_y
- C_{22} – flexural stiffness of the section when the member is bent in the yz plane
- C_{23} – stiffness which takes into account the mutual influence of M_x and M_y
- C_{33} – flexural stiffness of the section when the member is bent in the xz plane
- e_m – diagram curvature parameter
- E – initial modulus of elasticity
- E_c, E'_c – initial and secant modulus of elasticity of concrete, respectively

- E_{ps}, E'_{ps} – initial and secant modulus of elasticity of prestressed steel, respectively
 E_s, E'_s – initial and secant modulus of elasticity of nonprestressed steel, respectively
 f – stress
 f_c – stress in concrete
 f_s – stress in steel
 f_y – yield strength of mild steel
 $f_{0.2}$ – conditional yield strength of high strength steel determined by 0.2% set method
 f_{ci} – stress in the i th elementary cell of concrete
 f_{psk} – stress in the k th strand, wire or bar of the prestressed steel
 f_{sj} – stress in the j th nonprestressed steel bar
 \hat{f}_c – stress at the vertex of the stress-strain diagram of concrete under uniaxial compression
 \hat{f}_s – stress at the vertex of the stress-strain diagram of steel
 \hat{f}_{ct} – stress at the vertex of the stress-strain diagram of concrete under uniaxial tension
 $f_{ps,e}$ – effective prestress
 $f_{ps,el}, f_{s,el}$ – proportionality limit of prestressed and nonprestressed steel, respectively
 Δf_{psk} – increment of stress in prestressed steel from external load
 \mathbf{F} – force vector
 h – height of section
 kk – number of effective elementary cells of concrete in the section
 ℓ – span length of the structural concrete member
 mm – number of nonprestressed steel bars in the section
 M_x, M_y – bending moment in the yz and xz plane, respectively
 $\Delta M_x, \Delta M_y$ – increment of bending moment in the yz and xz plane, respectively
 M_u^{cal}, M_u^{exp} – theoretical and experimental ultimate moment, respectively
 nn – number of prestressed steel strands, wires, and bars in the section
 N – longitudinal (normal) force
 ΔN – increment of longitudinal force
 N_u^{cal}, N_u^{exp} – theoretical and experimental ultimate axial force, respectively
 $U^{(\ell)}$ – strain energy per unit length
 \mathbf{Z} – vector of a geometric space
 \mathbf{Z}_k – vector of error
 ϑ_m – coefficient of elasticity for the material
 ϑ_o – coefficient of elasticity at the start of the stress-strain diagram of material
 $\vartheta_{0.2}$ – coefficient of elasticity of steel corresponding to the stress $f_{0.2}$ and strain $\varepsilon_{0.2}$
 β_{el} – coefficient of proportional limit, that is constant within the limits of reinforcement's grade
 γ – shear strain
 ε – strain
 $\hat{\varepsilon}_c$ – strain corresponding to the stress at the vertex of the stress-strain diagram of concrete under uniaxial compression
 $\hat{\varepsilon}_{ct}$ – strain corresponding to the stress at the vertex of the stress-strain diagram of concrete under uniaxial tension
 ε_o – axial strain at the chosen reference point O
 $\hat{\varepsilon}_s$ – steel strain corresponding to the stress at the vertex of the stress-strain diagram
 $\varepsilon_{0.2}$ – strain corresponding to the proof stress $f_{0.2}$ of high strength steel
 λ – strain vector
 λ_{i-1} – strain vector at the $(i-1)$ th iteration step

- λ_i – strain vector at the i th iteration step
 λ_y – the length of the yielding plateau
 τ – shear stress
 Ψ_x, Ψ_y – curvature of the member longitudinal axis in the yz and xz plane, respectively
 $\Omega_c, \Omega_{ps}, \Omega_s$ – region occupied by concrete, prestressed steel, and nonprestressed steel, respectively

References

- [1] ACI Committee 318 (2019): *Building code requirements for structural concrete (ACI 318-19): an ACI standard: commentary on building code requirements for structural concrete (ACI 318R-19): an ACI report.*– American Concrete Institute.
- [2] AASHTO, LRFD. (2012): *AASHTO LRFD bridge design specifications.*– American Association of State Highway and Transportation Officials, Washington, DC.
- [3] IBC, ICC. (2006): *International building code.*– International Code Council, Inc. (formerly BOCA, ICBO and SBCCI) 4051, 60478-5795.
- [4] CEN, Eurocode (2004): *2: Design of concrete structures. part 1-1: general rules and rules for buildings.*– CEN Comit Europen de Normalisation, Brussels.
- [5] BSI (1997): *Structural use of concrete, part 1. code of practice for design and construction.*– 8110-1.
- [6] AS3600, Australian Standard (2001): *Concrete structures, standards Australia.*– Sydney.
- [7] Standard, C. S. A. (2014): *Design of concrete structures–A23. 3-14.*– Mississauga: Canadian Standards Association.
- [8] Mörsch E.I. and Goodrich E.P. (1910): *Concrete-steel construction: (Der Eisenbetonbau).*– Engineering News Publishing Company.
- [9] Bebbly A.W. (1968): *Short-term deformations in reinforced concrete members.*– C & CA Technical Report, 42.408.
- [10] Jenn-Chuan C., You C. and Bazant Z.P. (1992): *Deformation of progressively cracking partially prestressed concrete beams.*– PCI Journal, vol.37, No.1, pp.74-85.
- [11] Alameh A.S. and Harajli M.H. (1989): *Deflection of progressively cracking partially prestressed concrete flexural members.*– PCI journal, vol.34, No.3, pp.94-128.
- [12] American Concrete Institute, and ACI Committee 224 (2001): *Control of cracking in concrete structures-ACI 224R-01.*– American Concrete Institute-ACI
- [13] Euro-International Committee for Concrete and Renaud Favre (1985): *CEB design manual on cracking and deformations.*– Ecole Polytechnique Fédérale de Lausanne.
- [14] Ng P.L., Lam J.Y. and Kwan A.K. (2010): *Tension stiffening in concrete beams. Part 1: FE analysis.*– Proceedings of the Institution of Civil Engineers: Structures and Buildings.
- [15] Nilson A.H. (1976): *Flexural stresses after cracking in partially prestressed beams.*– PCI Journal, vol.21, No.4, pp.72-81.
- [16] Branson D.E. and Trost H. (1982): *Unified procedures for predicting the deflection and centroidal axis location of partially cracked nonprestressed and prestressed concrete members.*– PCI Journal, vol.79, No.2, pp.119-130.
- [17] Branson D.E. and Trost H. (1982): *Application of the I-effective method in calculating deflections of partially prestressed members.*– PCI Journal, vol.27, No.5, pp.62-77.
- [18] Tadros M.K. (1982): *Expedient Serviceability Analysis of Cracked Prestressed Concrete Beams.*– PCI Journal, vol.27, No.6, pp.67-86.
- [19] Bazant Z.P. and Byung H.O. (1984): *Deformation of progressively cracking reinforced concrete beams.*– PCI Journal, vol.81, No.3, pp.268-278.
- [20] Tadros M.K., Ghali A. and Arthur W.M. (1985): *Prestress loss and deflection of precast concrete members.*– PCI Journal, vol.30, No.1, pp.114-141.
- [21] Kawakami M., Tokuda H., Kagaya M. and Hirata M. (1985): *Limit states of cracking and ultimate strength of arbitrary concrete sections under biaxial loading.*– PCI Journal, vol.82, No.2, pp.203-212.
- [22] Ghali A. (1993): *A Critical Review.*– Structural Journal, vol.90, No.4, pp.364-373.
- [23] Kawakami M. and Ghali A. (1996): *Time-dependent stresses in prestressed concrete sections of general shape.*– PCI Journal, vol.41, No.3, pp.96-105.
- [24] Kawakami M. and Ghali A. (1996): *Cracking, ultimate strength and deformations of prestressed concrete sections of general shape.*– PCI Journal, vol.41, No.4, pp.114-122.
- [25] Mast R.F. (1998): *Analysis of cracked prestressed concrete sections: A practical approach.*– PCI Journal, vol.43, No. 4, pp.80-91.

- [26] Bischoff P.H. (2005): *Reevaluation of deflection prediction for concrete beams reinforced with steel and fiber reinforced polymer bars.*– Journal of Structural Engineering, vol.131, No.5, pp.752-767.
- [27] Bischoff P.H. (2007): *Rational model for calculating deflection of reinforced concrete beams and slabs.*– Canadian Journal of Civil Engineering, vol.34, No.8, pp.992-1002.
- [28] Bischoff P.H. and Scanlon A. (2007): *Effective moment of inertia for calculating deflections of concrete members containing steel reinforcement and fiber-reinforced polymer reinforcement.*– ACI Structural Journal, vol.104, No.1, pp.68.
- [29] Scordelis A.C. (1984): *Computer models for nonlinear analysis of reinforced and prestressed concrete structures.*– PCI Journal, vol.29, No.6, pp.116-135.
- [30] Oukaili, N.K. (1991): *Strength of partially prestressed concrete elements with mixed reinforcement by highly strength strands and steel bars.*– Ph.D. dissertation, Moscow Civil Engineering University, Moscow, Russia.
- [31] Popovics S. (1970): *A review of stress-strain relationships for concrete.*– ACI Journal, vol.67, No.3, pp.243-248.
- [32] Naaman A.E. (1983): *An approximate nonlinear design procedure for partially prestressed concrete beams.*– Computers and Structures, vol.17, No.2, pp.287-299.
- [33] Karpenko N.I., Mukhamediev T.A. and Petrov A.M. (1986): *Initial and transformed deformation diagrams for concrete and steel.*– Stress-Strain State of Concrete and Reinforced Concrete Construction, NIIZHB, pp.7-25.
- [34] Karpenko N.I., Eryshev V.A. and Latysheva E.V. (2015): *Stress-strain diagrams of concrete under repeated loads with compressive stresses.*– Procedia Engineering, vol.111, pp.371-377.
- [35] Douglas F.J. and Burden R. (1998): *Numerical methods.*– Cole, 2nd ed., Pacific Grove, CA, USA.
- [36] Dodonov M.I., Golovin N.G., Oukaili N.K. and Kunishev V.K. (1992): *Strength and stress-strain condition of reinforced concrete elements.*– Special Report, Bulletin No.11232, VNIINTPI, Moscow, Russia, p.32.
- [37] Dodonov M.I., Frolov A.K. and Kim L.V. (1987): *Strength of normal sections of eccentrically compressed reinforced concrete elements with high-strength steel.*– Construction and Architecture Journal, No.7, pp.1-5.
- [38] Bajkov V.N., Dodonov M.I., Rastorguev B.S., Frolov A.K., Mukhamediev T.A. and Kunizhev V.K. (1987): *General case of elements strength calculation proceeding from normal sections.*– Concrete and Reinforced Concrete Journal, vol.386, No.5, pp.16-18.
- [39] Bajkov V.N., Dodonov M.I., Rastorguev B.S., Frolov A.K., Mukhamediev T.A. and Kunizhev V.K. (1988): *Calculation of the strength of normal section of skew eccentrically compressed reinforced concrete elements.*– Studies on the Substantiation of Strength and Durability of Concrete and Reinforced Concrete Constructions of Power Structures, IZVESTIJA VNIIG, vol.204, pp.42-47.

Received: September 1, 2020

Revised: December 2, 2020